MATEHEMATIC MORPHOLOGY APPROACH FOR RENAL BIOPSY ANALYSIS

Ferran Marqués, Gemma Cuberas, Antoni Gasull[1], Daniel Serón, Francesc Moreso[2], Nayana Joshi[3]

[1]Technical University of Catalonia
(UPC) Barcelona, SPAIN
{ferran, gasull}@gps.tsc.upc.es
http://gps-tsc.upc.es/imatge/

[2]Department of Nephrology
Ciutat Sanitària i Universitària de Bellvitge
Bellvitge, SPAIN

[3]Department of Orthopedics Surgery
Hospital Universitari Vall d'Hebron
Barcelona, SPAIN

ABSTRACT

This paper proposes a new technique for the analysis of renal biopsies stained with Sirius red and digitized under non-polarized light. The renal interstitial space, the cortex area and the tubules should be segmented to allow the estimation of the renal cortical interstitial volume fraction and the parameters characterizing the tubule distribution. In this paper, a totally automatic algorithm is proposed that relies on mathematic morphology tools. The proposed algorithm has been assessed in a large number of biopsies leading to similar results to those obtained by the manual approach.

1. INTRODUCTION

This paper proposes a new technique for the analysis of renal biopsies stained with Sirius red and digitized under non-polarized light. The renal interstitial space, the cortex area as well as the tubules should be segmented to allow the estimation of the renal cortical interstitial volume fraction and the parameters characterizing the tubule distribution.

The estimation of the interstitial space is usually performed either manually (point-counting technique) or using semi-automatic algorithms that require several correction steps, being both approaches very tedious and time consuming. Previous techniques for automatic [1] or semiautomatic [2, 3] quantification of interstitial areas and tubules morphometry have rely on morphological tools [4]. Nevertheless, the results of these techniques are not fully satisfactory since they require very strict conditions in the staining process or a non-negligible amount of human interactions. In this paper, a totally automatic algorithm is proposed. It relies on mathematic morphology tools which take advantage of the different visual features of the various elements to be segmented in the image.

Figure 1 presents two typical examples of non-polarized Sirius red stained renal biopsies. Red structures in Figure 1 correspond to the renal interstitial space. In regular areas of the tissue, the renal interstitial space mainly corresponds to the walls of the tubules. However, in some areas, renal interstitial damage can be observed in terms of tubular atrophy and interstitial widening. These areas in which the tubular distribution is not regular have to be computed as interstitial zone, in spite of not forming a homogenous, dense tissue.

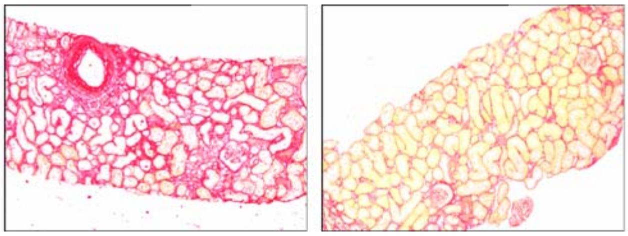

(a) (b)

Figure 1: (a) Original image. (b) Original image.

The paper is structured as follows. After this brief introduction, Section 2 details the main steps of the analysis algorithm. To illustrate the various steps, partial results of the algorithm when applied to the image in Figure 1.a are interleaved with the algorithm description. For presentation purposes, the inverse images are shown throughout the complete paper. Section 3 discusses the results and, finally, Section 4 presents the conclusions and current work.

2. ANALYSIS ALGORITHM

The proposed technique deals with the non-polarized version of the Sirius red stained renal biopsies. The algorithm can be divided into three main steps:

- Pre-processing including a colour transformation and a simplification step.
- Image segmentation based on an adaptive threshold.
- Segmentation refinement using an area filter and the watershed algorithm.

In the sequel, these three main steps are detailed.

2.1 Pre-processing

Non-polarized Sirius red stained renal biopsies present a colour distribution that allows the application of a simple colour transformation which preserves the interstitial information. This way, the image is transformed from a 3D space (*RGB*) to a 1D space (*I*) and the complete segmentation process is carried out on this new image. The used transform is given by:

$$I = \begin{cases} R-G & if\, R-G>0 \\ 0 & if\, R-G \le 0 \end{cases}$$

Figure 2 presents the results of the pre-processing step. In Figure 2.a, it can be observed the fact that all the original structures are correctly preserved by the colour transform. On this image, and in order to homogenize the damaged interstitial areas, a simplification step is applied. The selected filter is a closing by reconstruction (φ^{rec}) [4] and its effect is illustrated in Figure 2.b. The behaviour of the filters by reconstruction is discussed in the next subsection in a simpler (binary) case.

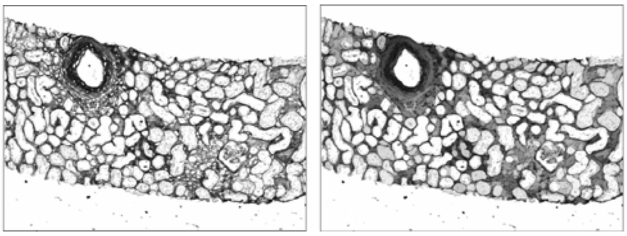

(a) (b)

Figure 2: (a) Colour transformation. (b) Simplification step. (For illustration purposes, inverse images are presented)

The size of the structuring element used in the filtering process depends on the image resolution. The filter should homogenize the damaged interstitial areas while preserving the tubules. For this image magnification, the filter size has been set by the physicians to 7x7 pixels.

2.2 Image segmentation

2.2.1 Basic principles

The segmentation algorithm is based on the morphological operator opening by reconstruction (γ^{rec}). This operator, applied on binary images, allows the perfect reconstruction of those connected components in a reference image which have been selected in a marker image. In this work, pixels in connected components are set to 255 (0 in the images). In this context, a component in the reference image (R) is said to be selected if at least one of its collocated pixels in the marker image (M) is set to 255. The implementation of this operator is given by the following expression:

$$\gamma^{rec}(R,M) = \bigcup_n \delta_R^{(n)}(M)$$

in which $\delta_R^{(n)}(X)$ represents the geodesic dilation of the set M within the reference R with a ball of size n.

The opening by reconstruction operator allows the implementation of adaptive threshold techniques. The reference image is created by imposing an unrestrictive threshold that preserves the complete desired structure (the interstitial area) but may include some other elements (some areas within the tubules). In turn, the marker image is created by using a more restrictive threshold that only preserves a partial representation of the desired structure. The opening by reconstruction will reconstructed the complete interstitial zone while removing the elements in the tubule interior.

2.2.2 Threshold selection

In this application, the unrestrictive threshold can be obtained as an estimation of the image background value of the simplified image (S). This estimation is found by performing an opening of the image with a large structuring element that removes all the structure information (interstitial zone). The background value is estimated by the median value of the resulting image. In order to speed up the algorithm, the opening is not performed over the complete image but only in a few image lines (typically, three).

The more restrictive threshold is obtained as an estimation of the interstitial value. Initially, the dual operation of the previous one is performed: a closing with a large structuring element that removes all the background information. The median value of the resulting image (m) provides with a first estimate of the interstitial zone.

To improve the estimation of this parameter, a top-hat transform (τ) with a small opening by reconstruction (5x5 pixels structuring element) is performed on S:

$$\tau(S) = S - \gamma^{rec}(S,S)$$

The top-hat transform detects all the small, bright components in the image; that is, the interstitial zone as well as noisy bright peaks in the image. To compute a robust estimate of the interstitial value, all peaks preserve by the top-hat having a grey level value larger than m in the original image are kept. The restrictive threshold is obtained by computing the mean value of the remaining peaks.

The results of these operations are presented in Figures 3 and 4. Figure 3 shows the selection of the interstitial areas that will be used in the estimation of the restrictive threshold. The removal of all thin, bright components is presented in Figure 3.a, whereas Figure 3.b shows the selected areas. Note that only a few wrong pixels are preserved in this image which allows a very robust foreground level estimation.

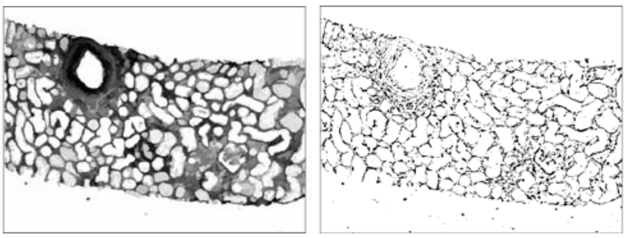

(a) (b)

Figure 3: (a) Opening by reconstruction. (b) Selected areas.

In turn, Figure 4 shows the binarization results obtained using both thresholds. Figure 4.a presents the result of the less restrictive threshold. It can be seen that the selected structures are almost a superset of the desired structures (the interstitial area). Figure 4.b presents the result of the more restrictive threshold. As expected, the result is a subset of the desired structures.

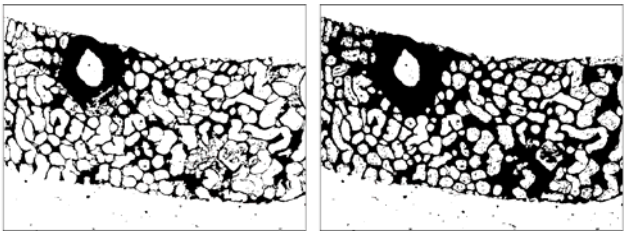

(a) (b)

Figure 4: (a) Restrictive and (b) unrestrictive binarizations.

2.2.3 *Final segmentation*

As previously commented, the two binary images are combined using an opening by reconstruction to obtain the final interstitial zone. The result is presented in Figure 5, where the original image is also shown for comparison purposes.

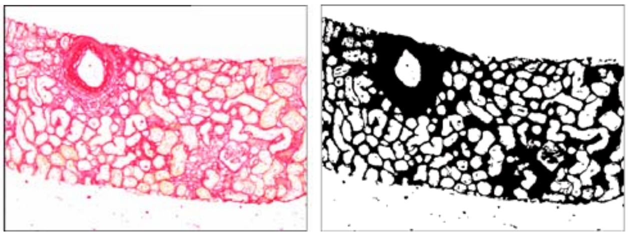

(a) (b)

Figure 5: (a) Original image. (b) Interstitial area.

2.3 Segmentation refinement

As shown if Figure 5.b, the segmentation of the interstitial area is very accurate. It has to be noticed that the proposed technique is able to cope at the same time with very fine structures (as the tubular walls) and segment the damaged interstitial areas in spite of their heterogeneous textures. The final segmentation (that is, the assignment of a single label to all the interstitial area and a different label to every tubule) can be easily obtained from this result since the objects are (almost in all cases) represented by individual connected components.

Nevertheless, further improvement is still possible since segmentations may present two problems:

- Some isolated, small components are classified as being part of the interstitial area.
- A few tubular walls are not completely detected and pairs of tubules may be merged into a single component.

The first problem can be easily solved by means of an area filter, which removes all connected components smaller that a given value.

In order to solve the second problem, a marker-based watershed algorithm has been applied [4, 5]. In this technique, all regions in the previous segmentation representing tubules are eroded. Erosion will divided into two different connected components those regions representing two tubules that have been merged due to the lack of detection of part of their wall. On the other hand, those connected components representing a single tubule will only be shrunk, due to the smooth shape of tubules. This way, after erosion, every tubule is represented by a single connected component which is used as a marker in the watershed process.

The marker-based watershed can be understood as a region growing algorithm. In this application, all the regions representing the tubules as well as the region representing the interstitial zone are grown to cover the uncertainty area that has been created when eroding the initial tubule regions. The growing process can be performed taking into account any local features of the image. In this application, the grey level values of the simplified image (*S*) have been used.

The result of this process is presented in Figure 6. For illustrating this step, since the image in Figure 1.a did not present very relevant problems in this aspect, we have used the image in Figure 1.b. In Figure 6, it can be seen that, although the pixel values on some areas of the tubule wall are so low that they cannot be correctly segmented (see Figures 6.a and 6.b), the use of the marker-based watershed approach allows the system to recover from these errors (Figure 6.c). The final interstitial segmentation is presented in Figure 7.a.

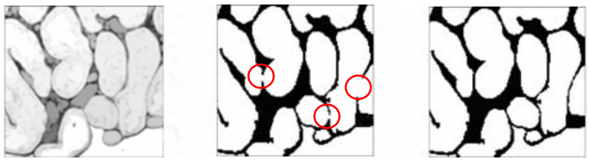

(a) (b) (c)

Figure 6: (a) Zoom on the simplified image. (b) Tubular walls not detected. (c) Final interstitial segmentation

2.4 Cortex segmentation

Finally, in order to estimate the renal cortical interstitial volume fraction, the complete cortex area has to be computed. This result can be easily obtained from the final segmentation achieve in the previous step. An opening by reconstruction is applied using as reference image the interstitial segmentation and as marker image an image with only the frame (the whole image set to 255 and the frame set to 0). The fact of using the frame as a marker ensures that tubules partially represented in the biopsy are removed from the final cortex area, as it can be seen in the cortex segmentation presented in Figure 7.b.

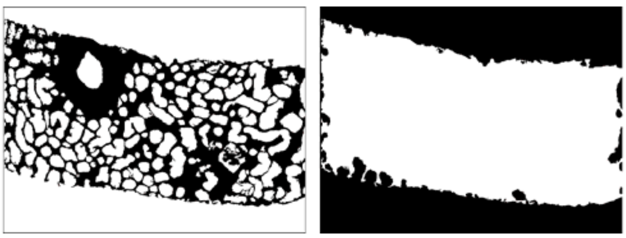

(a) (b)

Figure 7: (a) Interstitial and (b) Cortex segmentation.

3. RESULTS

The proposed algorithm has been assessed in a large number of biopsies leading to similar results to those obtained by the manual approach. In this section, the typical results are commented based on the analysis of four different images.

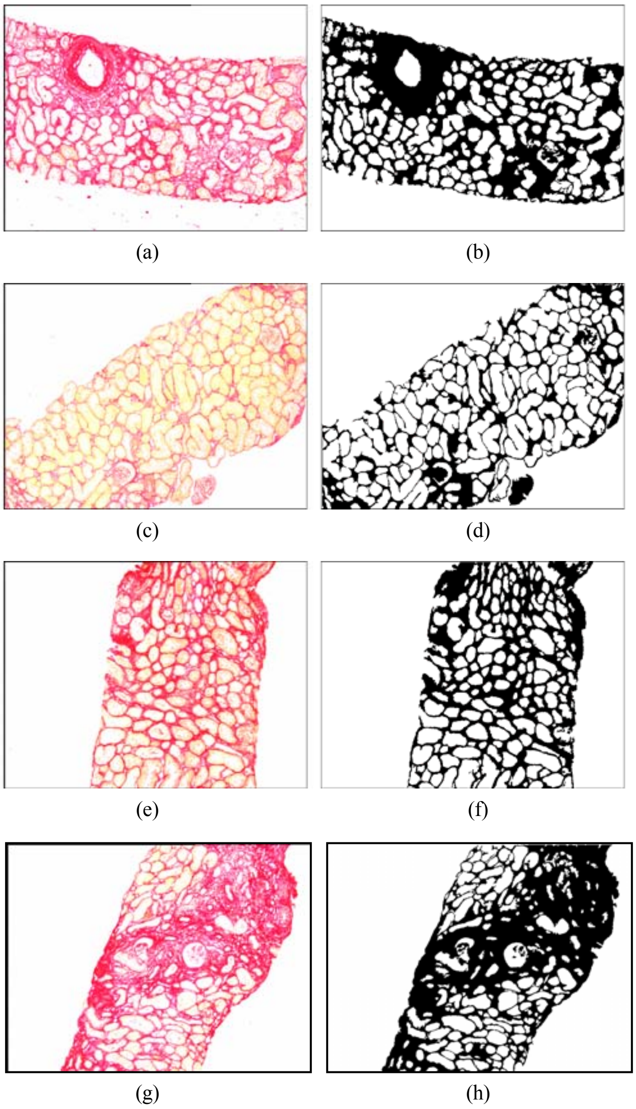

Figure 8: (a, c, e, g) Original images. (b, d, f, h) Interstitial segmentations.

The results shown in Figure 8 assess the robustness of the proposed system with respect to the various possible scenarios. The four examples represent different staining and illumination conditions that lead to a variation of the basic colours present in the biopsy. In spite of that, the final results are correct which validates the pre-processing step and, concretely, the colour transformation.

In addition, the degree of damaged interstitial areas and their type (texture and homogeneity) largely differs among the various images. Nevertheless, the final interstitial segments are well defined which demonstrate the correct selection of the methodology and, specifically, the correct choice of the filter sizes.

Finally, it has to be highlighted that the presence of elements in the biopsy which are neither interstitial area nor tubules is correctly handled by the algorithm. This way, the presence of a vase in Figure 8.a and of glomeruli in Figures 8.c and 8.g are accurately classified.

4. CONCLUSIONS AND CURRENT WORK

The proposed technique has been successfully tested on the database of renal biopsies of the Department of Nephrology of the *Ciutat Sanitària i Universitària de Bellvitge*. Currently, the method is being tested using the databases of other institutions to assess its compatibility. The goal is to develop a protocol for the creation of such biopsies (type of illumination, magnification, staining process …) that will minimize the risk of their automatic analysis.

In addition, extensions of this technique have being conducted to complete the study of the Sirius red stained biopsy database. This way, the polarized light versions of the databases have been analyzed to compute either additional parameters or to further verify the obtained ones [6].

Finally, we are currently developing classification techniques in order to determine the presence of other elements apart from tubules in the biopsy (typically vases and glomeruli).

5. ACKNOWLEDGMENTS

The work presented in this paper has been partially supported by the grant TIC2001-0996 of the Spanish Government.

REFERENCES

[1] D. Serón et al., “Automated classification of renal interstitium and tubules by local texture analysis and a neural network”. Analytical and Quantitative Cytology and Histology 1996; vol. 18:410 -419.

[2] M. Masseroli et al., “Design and validation of a new image analysis method for automatic quantification of interstitial fibrosis and glomerular morphometry”. *Laboratoty Investigation* 1998; Vol. 78:511-522.

[3] F. Moreso et al., “Quantification of interstitial chronic renal damage by means of texture analysis”, *Kidney International*, Vol. 46, pp. 1721-1727, 1994.

[4] P. Soille, *Morphological Image Analysis: Principles and Applications*, Springer Verlag, June 1999.

[5] S. Beucher and F. Meyer, “The Morphological approach of segmentation: the watershed transformation”, In Dougherty E. (Editor), *Mathematical Morphology in Image Processing*, Marcel Dekker, New York, 1992.

[6] A. Gasull et al., “Renal Interstitium and tubules detection using mathematic morphology tools”, Submitted to BIOSIGNAL 2004, Brno, July 2004.